

The Ioffe-Regel criterion and diffusion of vibrations in random lattices

Y. M. Beltukov and V. I. Kozub
A. F. Ioffe Physical-Technical Institute, 194021 Saint Petersburg, Russia

D. A. Parshin
Saint Petersburg State Polytechnical University, 195251 Saint Petersburg, Russia
(Dated: August 11, 2022)

We consider diffusion of vibrations in 3d random harmonic lattices with translational invariance. Above some frequency ω_{IR} , corresponding to the Ioffe-Regel crossover, notion of phonons becomes ill defined. They cannot propagate through the lattice and transfer energy. Nevertheless most of the vibrations in this range are not localized. We show that they are similar to *diffusons* introduced by Allen, Feldman et al., Phil. Mag. B **79**, 1715 (1999) to describe heat transport in glasses. The crossover frequency ω_{IR} is close to the position of the boson peak. Changing strength of disorder we can vary ω_{IR} from zero value (when rigidity is zero and there are no phonons in the lattice) up to a typical frequency in the system. Above ω_{IR} the energy in the lattice is transferred by means of diffusion of vibrational excitations. We calculated the diffusivity of the modes $D(\omega)$ using both the direct numerical solution of Newton equations and the formula of Edwards and Thouless. It is nearly a constant above ω_{IR} and goes to zero at the localization threshold. We show that apart from the diffusion of energy, the diffusion of particle displacements in the lattice takes place as well. Above ω_{IR} a displacement structure factor $S(\mathbf{q}, \omega)$ coincides well with a structure factor of random walk on the lattice. As a result the vibrational line width $\Gamma(q) = D_u q^2$ where D_u is a diffusion coefficient of particle displacements. Our findings may have important consequence for the interpretation of experimental data on inelastic x-ray scattering and mechanisms of heat transfer in glasses.

PACS numbers: 63.50.-x, 65.60.+a, 78.70.Ck

I. INTRODUCTION

Propagation of vibrational excitations in disordered systems is one of the advanced problems in condensed matter physics. In particular, transport mediated by these excitations is responsible for the thermal conductivity of amorphous dielectrics (glasses). However mechanisms of heat transfer in glasses above the plateau region are still poorly understood.

At low temperatures below 1 K the low frequency plane long wave acoustical phonons are well defined excitations which transfer the heat in glasses. At these temperatures the thermal conductivity $\kappa(T) \propto T^2$ and is controlled by a resonant scattering of phonons on two-level systems (TLS)^{1,2}. Between 4 K and 20 K the thermal conductivity $\kappa(T)$ saturates and displays a well known plateau³. As was shown in⁴ it can be explained by resonant scattering of phonons by quasilocal vibrations (QLV). The QLV, together with TLS and phonons are vibrational excitations responsible for many universal properties of glasses⁵.

However, above approximately 20 K the thermal conductivity rises again and finally saturates on the level of one order of magnitude higher, i.e. at temperatures about several hundreds Kelvin⁶. As generally believed, the origin of this second rise of the thermal conductivity (above the plateau) is not related to phonons. It was established long ago⁷⁻⁹, that in this temperature (frequency) range the mean free path of phonons l becomes of the order of their wave length λ (or even smaller, of the order of interatomic distance). Corre-

spondingly, the Ioffe-Regel criterion for phonons¹⁰ becomes violated. The existence of such crossover was confirmed by molecular dynamics calculations for some real and model glasses^{11,12} and disordered lattices^{13,14}.

In the regime of such strong scattering a standard concept of plane waves (phonons) with a well defined wave vector \mathbf{q} becomes inapplicable. The question then arises: what physical mechanism is responsible for the heat transfer in glasses in this temperature range? The numerical simulations show that majority of the vibrational modes in the corresponding frequency range are not localized¹⁵⁻¹⁷.

As was shown in¹⁸⁻²⁰, a lower limit of the thermal conductivity of amorphous solids above 30 K can be correctly estimated within the framework of the Einstein's model²¹. It was assumed that the mechanism of heat transport above the plateau is a random walk of thermal energy between clusters of neighboring atoms vibrating with random phases. In fact, a diffusion mechanism for the heat transfer in this temperature range was proposed.

At the same time, delocalized vibrations in glasses of a new type, different from phonons, were introduced. They were called *diffusons*²²⁻²⁶. These are vibrations spreading through the system not ballistically, as phonons (on distances of the order of mean free path) but by means of diffusion. It is an important class of excitations which occupy in glasses the dominant part of the spectrum²⁶. In these papers it was put forward the hypothesis that the boundary between phonons and diffusons is determined by the Ioffe-Regel criterion for phonons. Since diffusons are delocalized excitations, they may be responsible for the thermal conductivity of glasses above the plateau.

The similar conclusion was made by the authors of^{27,28}. They considered the case of strong scattering of phonons in disordered lattices with a significant fraction of randomly located missing sites, but which is still far from the percolation threshold. It was shown that, in contrast to the electronic case, the Ioffe-Regel criterion is inaccurate in the prediction of phonon localization. Instead of localization, the vibrational transport above the Ioffe-Regel threshold becomes diffusive with approximately constant energy diffusivity $D(\omega)$. The diffusivity was calculated by numerical solution of the Newton equations for particle displacements. Similar calculations but for real glasses were done in the papers^{29,30} using molecular dynamics methods.

The diffusons above the Ioffe-Regel crossover were identified also in granular jammed systems with repulsive forces between the particles^{31,32}. They also have diffusivity which is independent of frequency ω . It was calculated making use of the Kubo-Greenwood formula for the thermal conductivity derived in²³. In jammed systems the Ioffe-Regel crossover frequency ω_{IR} can vary. It is shifted to zero when the system approaches the jamming transition point.

Therefore, as we believe, it is important to study properties of diffusons systematically in systems where they exist. They bring a new physics to our understanding of vibrational properties in strongly disordered systems and energy/heat transfer in glasses. As is well known the number of diffusing physical quantities coincides with the number of integrals of motion. Besides energy, we have two quantities which are conserved in a disordered closed mechanical system which is not affected by external forces. These are the total momentum and the position of the center of inertia. Since they are connected with each other, it should exist at least one new additional diffusion coefficient, different from the energy diffusivity $D(\omega)$ investigated in²²⁻²⁶. We show in this paper that this new coefficient is a *diffusivity of particle displacements*, D_u .

To study these important properties we should have a model, sufficiently simple, to describe all of them. Recently, using a random matrix approach, we developed a simple scalar model of a 3d disordered harmonic lattice with translational invariance which, as we believe, can represent typical properties of vibrations in disordered systems^{33,34}. It was shown that for a certain type of disorder the rigidity of the system is zero and the usual phonons (plane waves) cannot propagate through the lattice. However almost all vibrations in the lattice are delocalized and therefore can participate in the heat transfer. As we will show in the present paper they are similar to diffusons introduced in²⁶.

One can continuously bring rigidity and phonons back to the lattice increasing the width of the so-called *phonon gap*³⁴. It is a region where density of vibrational states $g(\omega) \propto \omega^2$. We will show that in this gap phonons are well defined plane wave excitations. However above the gap they cease to exist, since their mean free path be-

comes of the order of wave length what corresponds to the Ioffe-Regel crossover.

Nevertheless vibrations outside the gap remain delocalized and can participate in the heat transfer. Similar to the case of zero rigidity the character of the energy transfer in this frequency range is diffusive and is drastically different from the ballistic phonon mechanism. We believe that in this case vibrational properties of our system may be similar to the properties of real glasses. Therefore we are going to consider in more details properties of phonons and diffusons in these disordered lattices. To start with, for the sake of clarity of further consideration, we outline below the main properties of our model.

II. A RANDOM MATRIX APPROACH

The vibrational properties of a mechanical system of N particles are determined by the dynamical matrix $M_{ij} = \Phi_{ij}/\sqrt{m_i m_j}$, where Φ_{ij} is the force constant matrix and m_i are the particle masses. The matrices M and Φ are real, symmetric and *positive definite* matrices $N \times N$ (we consider for simplicity a scalar model). The last condition is important. It ensures mechanical stability of the system.

One can always present every real, symmetric and positive definite matrix M in the following form^{35,36}

$$M = AA^T, \quad \text{or} \quad M_{ij} = \sum_k A_{ik} A_{jk}. \quad (1)$$

Here A is some real matrix of a general form (not necessarily symmetric). And, vice versa, for every real matrix A the product AA^T is always a positive definite symmetric matrix.

For a free mechanical system it is necessary to satisfy also *translation invariance* conditions

$$\sum_i M_{ij} = \sum_j M_{ij} = 0 \quad (2)$$

(for simplicity we consider below all masses $m_i = 1$). It ensures that the potential energy of the system depends only on the differences of particle displacements.

We believe that some important properties of glasses can be reproduced if we take matrix A as a random one. As in³⁴, we consider the case of a simple cubic lattice with N particles and lattice constant $a_0 = 1$. Each particle has its unique integer index i which takes values from 1 to N . We construct the matrix A as follows. The non-diagonal elements A_{ij} (for $i \neq j$) we take as independent random numbers from Gaussian distribution with zero mean $\langle A_{ij} \rangle = 0$ and unit variance $\langle A_{ij}^2 \rangle = 1$ if i -th and j -th particles are nearest neighbors. For each particle in a simple cubic lattice there are six nearest neighbors. Non-diagonal elements A_{ij} and A_{ji} are statistically independent from each other (matrix A is non-symmetric). All other non-diagonal elements (for non-nearest neighbors) $A_{ij} = 0$. To ensure the translational invariance the

diagonal elements A_{ii} are calculated as follows

$$A_{ii} = - \sum_{j \neq i} A_{ji}. \quad (3)$$

Then, according to Eq. (1), the Eq. (2) will be also met.

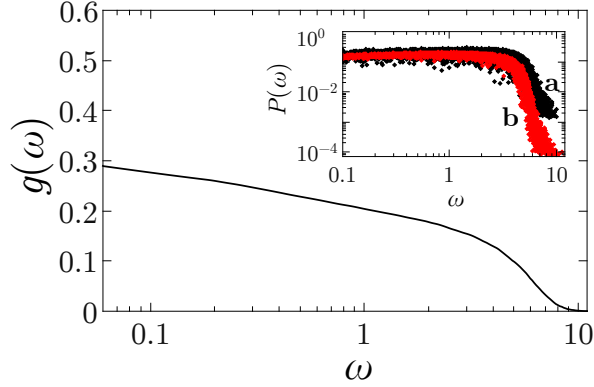


FIG. 1: The normalized DOS $g(\omega)$ for random matrix $M = AA^T$ built on a simple cubic lattice with $N = 20 \times 20 \times 20$ particles and averaged over 1000 realizations. Inset: The participation ratio $P(\omega)$ for $N = 10^3$ (a) and $N = 27^3$ (b) for one realization.

Fig. 1 shows the normalized density of vibrational states (DOS) $g(\omega)$ of matrix $M = AA^T$ in this cubic lattice. The periodic boundary conditions were used. As follows from the figure, $g(\omega)$ is nonzero at $\omega \rightarrow 0$. In spite of the presence of translational invariance we do not see the expected phonon modes with their DOS $g_{\text{ph}}(\omega) \propto \omega^2$ for $\omega \rightarrow 0$. It means that phonons as plane wave excitations cannot propagate through the lattice.

As was shown in³⁴ it is because the affine assumptions are violated and the macroscopic elasticity theory becomes inapplicable in this case. The average value of the Young modulus of the lattice $E \propto 1/N$. Therefore in the thermodynamic limit ($N \rightarrow \infty$) $E \rightarrow 0$. As a result the rigidity of the lattice and sound velocity are also zero. This unusual behavior is due to presence of high concentration of *negative springs* in the lattice which makes it extremely soft.

To determine whether vibrational modes are localized or delocalized we have calculated the participation ratio

$$P(\omega) = \left[N \sum_{i=1}^N e_i^4(\omega) \right]^{-1}. \quad (4)$$

Here $e_i(\omega)$ is i -th particle normalized eigenvector with frequency ω . As one can see from the inset of Fig. 1, all modes with exception of small high frequency part are *delocalized*. They have $P(\omega) \approx 0.2$ which is independent of the system size. This value is close to the theoretical value $1/3$ for Porter-Thomas distribution of $e_i^2(\omega)$ ^{33,37}. We have verified also that the level spacing distribution obeys the Wigner-Dyson statistics³³. It also indicates the mode delocalization. As we will show in Section IV, all

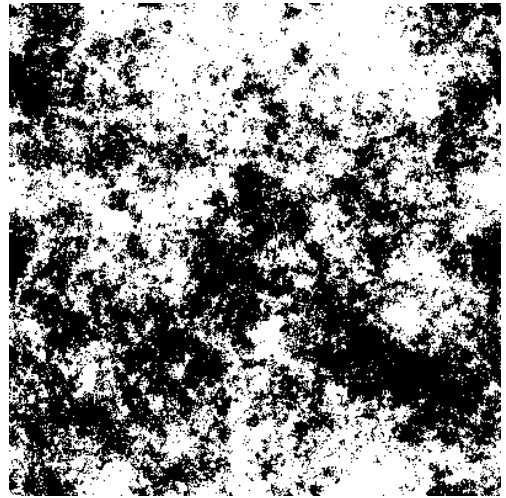


FIG. 2: The spacial eigenmode structure of random matrix $M = AA^T$ for the lowest frequency ω_{\min} in two dimensional square lattice 400×400 .

these delocalized vibrational modes can be identified as diffusons. They spread in the lattice by means of diffusion.

To elucidate a spacial structure of the eigenmodes for matrix $M = AA^T$ we considered as an example a two dimensional square lattice with $N = 400 \times 400$ particles and calculated eigenvector $e_i(\omega_{\min})$ ($i = 1, 2, \dots, N$) for the lowest frequency ω_{\min} in the system. The result is shown on Fig. 2. Particles with positive and negative displacements are shown by white and black dots correspondingly. As one can see from the figure, the mode is delocalized. Its spatial structure is random (fractal) and has nothing to do with a plane wave. Similar picture takes place in a 3d case.

III. PHONONS

To introduce phonons into the picture we should have finite rigidity of the lattice. Since a sum of positive definite matrices is a positive definite matrix then a possibility is to add to the random matrix AA^T a crystalline part³⁴

$$M = AA^T + \mu M_0. \quad (5)$$

Here matrix A is the same random matrix built on a 3d simple cubic lattice with translational invariance and $a_0 = 1$ as in the previous Section. Matrix M_0 is a positive definite crystal dynamical matrix for the same lattice with unit masses, and all spring constants (between the nearest neighbors) equal to unity. The tune parameter $\mu \geq 0$ controls the rigidity of the lattice.

To find the rigidity (as a function of μ) we calculated numerically the Young modulus E of the lattice with dynamical matrix given by Eq. (5) for $\mu \neq 0$. For that we fixed particles on the left hand side of our cubic sample

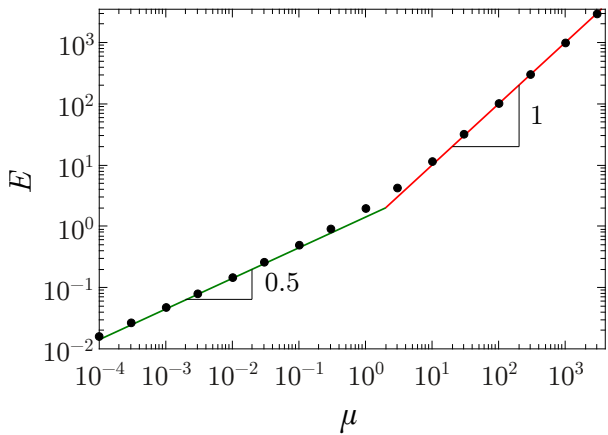


FIG. 3: Young modulus E as a function of μ for dynamical matrix $M = AA^T + \mu M_0$ built on a cubic lattice with $N = 100 \times 100 \times 100$ particles (one realization). Black dots are calculated values, the line is the best least-square fit.

with $N = L^3$ particles and displaced all particles on the opposite (right hand) side by the unit distance. In other two directions we used the periodic boundary conditions. Then, solving the system of linear Newton equations, we found the new equilibrium positions of all other particles in the sample and calculated restoring forces acting on the displaced particles on the right boundary. Due to randomness of the elastic bonds, the restoring forces are also random. Let \bar{f} be the average restoring force. Then the Young modulus E can be calculated as follows

$$E = \frac{\bar{f}}{L-1}. \quad (6)$$

To avoid confusion, we remind that we are using here a scalar version of the elasticity theory. Therefore all forces in the lattice are parallel (or antiparallel) to the particle displacements.

The results of these calculations are shown on Fig. 3 for cubic sample with $N = 10^6$ particles. As we can see from the fit, the Young modulus has a following dependence on μ :

$$E = \mu, \quad \mu \gg 1, \quad (7)$$

$$E = 1.5\sqrt{\mu}, \quad \mu \ll 1. \quad (8)$$

As a result, for $\mu \gg 1$ we have a usual crystal, where disorder is relatively small and relation (7) is obvious. For $\mu \ll 1$ the disorder is strong. The fluctuations of the nondiagonal matrix elements $M_{i \neq j}$ are bigger than the averaged values^{33,34}. In this case Young modulus $E \propto \sqrt{\mu}$. The origin of this behavior is unclear and it should be elucidated in future work. But we will support below our numerical findings by calculation of the sound velocity and the phonon density of states (for small ω) and comparison of the latter with total DOS calculated numerically for matrix (5).

To calculate the phonon contribution to the DOS at small ω , we need to know the sound velocity v at zero

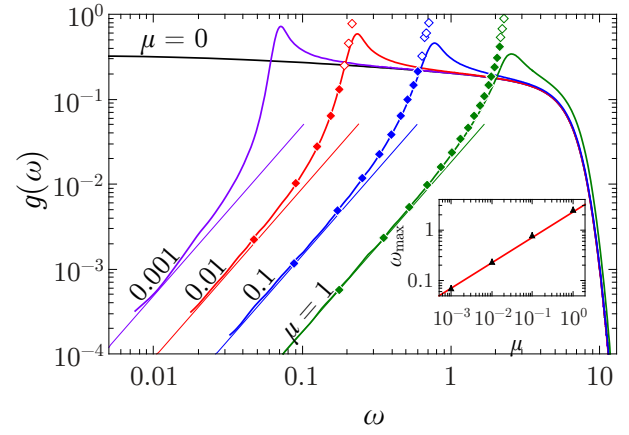


FIG. 4: The normalized DOS $g(\omega)$ for dynamical matrix $M = AA^T + \mu M_0$ and different μ (0, 0.001, 0.01, 0.1, 1) calculated with precise numerical KPM solution for cubic lattice with $N = 200^3$ (full lines). Straight lines correspond to Eq. (10) with sound velocity $v = \sqrt{E}$. Filled and open diamonds correspond to phonon contribution to the DOS below and above the Ioffe-Regel crossover frequency ω_{IR} correspondingly (see further text for details). Inset: dependence $\omega_{max}(\mu)$.

frequency. It is related to the Young modulus in a usual way:

$$v = \sqrt{E} \quad (9)$$

(since all particle masses $m_i = 1$ and lattice constant $a_0 = 1$). Then for the phonon DOS (in the scalar model) we have

$$g_{ph}(\omega) = \frac{1}{2\pi^2} \frac{\omega^2}{v^3}. \quad (10)$$

The total DOS $g(\omega)$, normalized to unity and calculated numerically by the kernel polynomial method (KPM)^{38,39} for dynamical matrix (5) for different values of $\mu \neq 0$ is shown on Fig. 4. We see from the figure that for finite values of $\mu \neq 0$ the DOS at low enough frequencies is proportional to ω^2 which corresponds to acoustical phonon excitations. Thus, introducing finite values of μ , we open in the vibrational spectrum a *phonon gap*. Just above this gap the DOS has a sharp maximum at frequency ω_{max} which we will identify with the width of the gap. As follows from the figure, the maximum frequency increases as $\omega_{max} \propto \sqrt{\mu}$.

Since the DOS $g(\omega)$ is normalized to unity, we conclude from the Fig. 4 that vibrations corresponding to the maximum for $\mu \neq 0$ were pushed out from the region of small frequencies $\omega < \omega_{max}$ for $\mu = 0$. As we will show further (see Table I), the frequency ω_{max} is correlated with position of the boson peak ω_b (the maximum in the reduced DOS $g(\omega)/\omega^2$). Therefore appearance of the boson peak in disordered systems is not necessarily related to the acoustic van Hove singularity in crystals as was proposed recently^{13,40,41}.

The straight lines on the Fig. 4 correspond to the phonon DOS $g_{\text{ph}}(\omega)$ determined by Eq. (10) with the sound velocity $v = \sqrt{E}$ and E calculated from Fig. 3. One can see a good agreement of the total $g(\omega)$ at low frequencies with the phonon contribution $g_{\text{ph}}(\omega)$. From that we can conclude that at least the low frequency excitations in the phonon gap are the usual long-wave phonons. However actually, as we will show further, nearly all excitations in the gap up to the frequencies close to ω_{max} belong to phonons but with a nonlinear dispersion law.

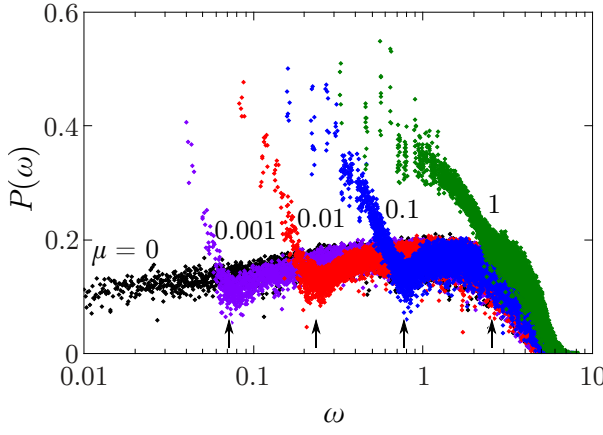


FIG. 5: Participation ratio for different μ as a function of ω for $N = 27^3$ (one realization). The arrows indicate positions of ω_{max} in $g(\omega)$ for corresponding values of μ (see Fig. 4).

This conclusion is supported by calculations of the participation ratio $P(\omega)$. It is shown in Fig. 5 for various values of μ . For $\mu \neq 0$ one can clearly distinguish in the function $P(\omega)$ two different frequency regions. As follows from Fig. 4, the low frequency part (below ω_{max}) corresponds to the phonons. In this range the participation ratio increases with decreasing frequency. It is related to increase of the phonon mean free path $l(\omega)$ as $\omega \rightarrow 0$ (see Fig. 9). In the high frequency part (above ω_{max}) $P(\omega)$ is approximately independent of the frequency and coincides with participation ratio for $\mu = 0$. As we will show in Section IV it corresponds to diffusons. A similar behavior of the participation ratio was found recently in 2d Lennard-Jones glasses⁴².

To find the phonon dispersion curve (dependence of the phonon frequency ω on the wave vector \mathbf{q}) and phonon mean free path $l(\omega)$ we should calculate space and time Fourier transform of the particle displacement field $u(\mathbf{r}, t)$. For that we ascribed to all the particles at the initial moment $t = 0$ random displacements (with Gaussian distribution with zero mean and unit variance) and zero velocities. Then, numerically solving Newton equations (using Runge-Kutta-4 method with the time step $\Delta t = 0.01$), we analyzed the particle dynamics at $t \neq 0$.

Let $u(\mathbf{r}_i, t)$ be the i -th particle displacement as a function of particle coordinate \mathbf{r}_i and time t . We define the displacement structure factor (DSF) of the displacement

field as follows

$$S(\mathbf{q}, \omega) = \frac{2}{NT} \left| \sum_{i=1}^N e^{-i\mathbf{q}\mathbf{r}_i} \int_0^T u(\mathbf{r}_i, t) e^{i\omega t} dt \right|^2. \quad (11)$$

For better frequency resolution the upper time limit T was taken sufficiently large ($T = 3000$), while the integration time step was chosen as $\Delta t = 0.01$. Since vectors \mathbf{r}_i in a cubic lattice are discrete, the wave vectors $\mathbf{q} \equiv \mathbf{q}_n$ are also discrete and are defined on the corresponding reciprocal lattice. For example, for cubic sample $L \times L \times L$ and $\mathbf{q} \parallel \langle 100 \rangle$ direction we have $q_n = 2\pi n/L$ where integer numbers n are $-L/2 \leq n \leq L/2$.

One can show that definition (11) is equivalent to the usual expression

$$S(\mathbf{q}, \omega) = \pi \sum_{j=1}^N \left| \sum_{i=1}^N e_i(\omega_j) e^{-i\mathbf{q}\mathbf{r}_i} \right|^2 \delta(\omega - \omega_j) \quad (12)$$

where it is written in terms of eigenvectors $e_i(\omega_j)$ and eigenfrequencies ω_j of matrix M . The density of states is related to the structure factor by the sum rule

$$g(\omega) = \frac{1}{\pi} \sum_{\mathbf{q}} S(\mathbf{q}, \omega). \quad (13)$$

According to definition (11) $S(0, \omega) = 0$ since the position of center of inertia is conserved and $\sum_i u(\mathbf{r}_i, t) = 0$.

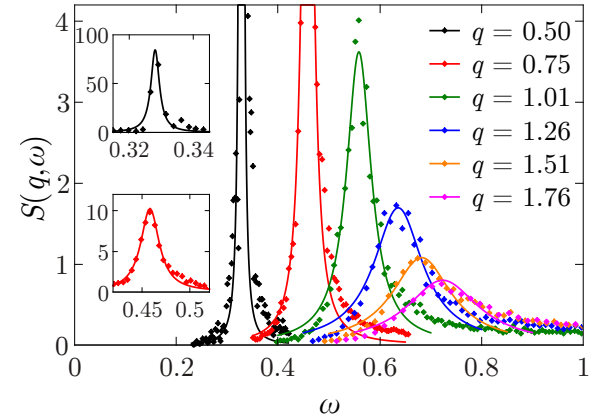


FIG. 6: The Lorentz dispersion curves for different wave vectors $\mathbf{q} \parallel \langle 100 \rangle$ direction and $\mu = 0.1$. Closed diamonds correspond to the calculated values of $S(\mathbf{q}, \omega)$ and lines are fitting curves according to Eq. (14). The number of particles $N = 50^3$ (one realization). Insets: the Lorentz dispersion curves for $q = 0.5$ and $q = 0.75$.

To analyze phonon excitations, we have found the maximum of $S(\mathbf{q}, \omega)$ as a function of ω for each discrete value of \mathbf{q}_n , for several values of μ . As an example, the results for $\mu = 0.1$ and one \mathbf{q} direction are shown on Fig. 6. For the fitting curves we used the Lorentz distribution

$$S(\mathbf{q}, \omega) \propto \frac{1}{(\omega - \omega_{\mathbf{q}})^2 + (\Delta\omega)^2}. \quad (14)$$

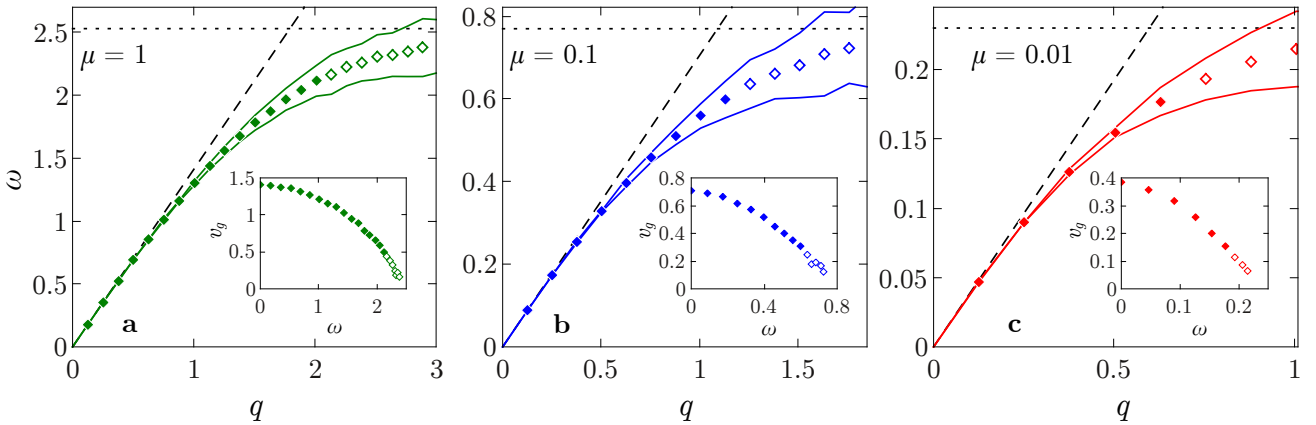


FIG. 7: The dependence ω_q on q for $\mathbf{q} \parallel \langle 100 \rangle$ direction for various μ (1, 0.1, 0.01) in a cubic sample with $N = 50^3$ (one realization). Filled and open diamonds are the maximums of $S(\mathbf{q}, \omega)$ as a function of ω for each discrete value of q_n for frequencies below and above the Ioffe-Regel crossover correspondingly (see text below for details). Solid lines correspond to halves of the maximums. Dashed lines show $\omega = vq$ linear dependence with sound velocity $v = \sqrt{E}$. Horizontal dotted lines correspond to the maximum frequency ω_{\max} in $g(\omega)$ (taken from Fig. 4). Insets show the group velocity $v_g = d\omega/dq$ as a function of ω .

From this fit we can find both the phonon frequency ω_q and the phonon line width $\Delta\omega$. The results for ω_q are shown on Fig. 7 for three values of μ and $\mathbf{q} \parallel \langle 100 \rangle$. For sufficiently small values of wave vector q we see a nice linear dispersion curve $\omega_q = vq$, with the sound velocity v given by Eq. (9). It is independent of the \mathbf{q} direction (i.e. the sound velocity is isotropic). With increase of q , the frequency ω_q shows a pronounced negative dispersion and approaches the maximum frequency ω_{\max} where the dependence ω_q saturates. In this \mathbf{q} region we observed a weak anisotropy of the dispersion curves for $\mu = 1$. At smaller values of μ the dependence ω_q is isotropic. Since $\omega_{\max} \propto \sqrt{\mu}$, the vertical axis on Fig. 7 scales approximately as $\sqrt{\mu}$ and the horizontal axis scales as $\mu^{1/4}$ (sound velocity $v \propto \sqrt{E} \propto \mu^{1/4}$, and $q_{\max} \approx \omega_{\max}/v$).

The strong negative dispersion in ω_q for big q values can be explained by *term crossing effect* due to the coupling of phonons to quasilocal vibrations near frequency ω_{\max} , corresponding to the sharp maximum in the DOS $g(\omega)$ (see Fig. 4). The dip in the participation ratio $P(\omega)$ for $\mu = 0.001$, $\mu = 0.01$ and $\mu = 0.1$ at $\omega \approx \omega_{\max}$ (see Fig. 5) evidences in favor of this idea. The vibrations inside the dip correspond to frequencies near ω_{\max} and have smaller participation ratio than the others. Therefore they can be referred to as quasilocal vibrations. In the following we will see that this strong scattering is also responsible for the deep minimum in the diffusivity $D(\omega)$ at $\omega \approx \omega_{\max}$ (see Fig. 17). Finally let us note that observed negative dispersion has nothing to do with the negative dispersion of transverse phonons in crystals near the Brillouin zone boundary.

The negative dispersion in ω_q is responsible also for the pronounced rise of the phonon DOS above the ω^2 dependence, given by Eq. (10). It is clearly seen on the Fig. 4. Indeed, taking the dispersion into account and disregarding weak anisotropy (taking place only for $\mu =$

1) we can write instead of Eq. (10)

$$g_{\text{ph}}(\omega) = \frac{1}{2\pi^2} \frac{q^2(\omega)}{v_g(\omega)}. \quad (15)$$

Here $v_g = d\omega/dq$ is the group velocity shown in Insets on Fig. 7. Taking for $q(\omega)$ and $v_g(\omega)$ the data from Fig. 7 we obtain the points (filled and open diamonds) shown on Fig. 4. Since they perfectly coincide with numerical data for $g(\omega)$ below ω_{\max} , we conclude that *all* the excitations in the phonon gap belong to phonons (with nonlinear dispersion at higher values of q).

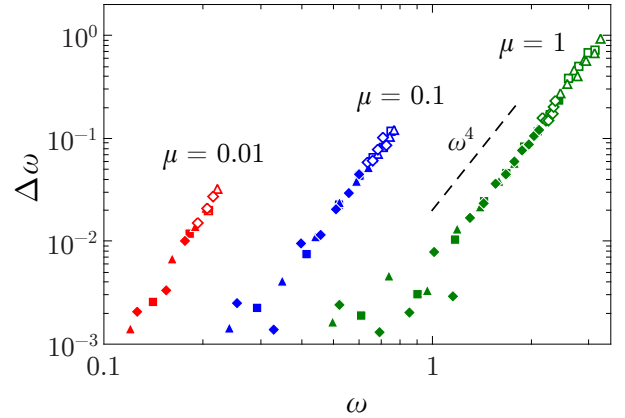


FIG. 8: The phonon line width $\Delta\omega$ as a function of ω for different μ in cubic sample with $N = 50^3$ (one realization). Different symbols correspond to different \mathbf{q} directions. \diamond for $\mathbf{q} \parallel \langle 100 \rangle$, \triangle for $\mathbf{q} \parallel \langle 110 \rangle$, \square for $\mathbf{q} \parallel \langle 111 \rangle$. Filled and open symbols refer to excitations below and above the Ioffe-Regel frequency ω_{IR} correspondingly (see text for details).

The phonon line width $\Delta\omega$ can be also found from fits similar to those shown on Fig. 6. It is related to the

phonon life time $\tau = 1/2\Delta\omega$. The factor 2 takes into account that $\Delta\omega$ corresponds to decay of the amplitude of the vibration. The results are shown on Fig. 8. As follows from this figure, $\Delta\omega \propto \omega^4$ and does not depend on the direction of \mathbf{q} . We think that this frequency dependence is not due to Rayleigh scattering of phonons on a static disorder. In such a case $\Delta\omega$ would be proportional to q^4 . Due to nonlinear dispersion in $\omega_{\mathbf{q}}$, these dependencies do not correspond to each other. More likely, the phonon line width is due to strong resonant scattering of phonons by quasilocal vibrations responsible for the sharp peak in the DOS, similar to those introduced in⁴. The deep minimum in the diffusivity $D(\omega)$ around frequency ω_{\max} also supports this idea (see Fig. 17). We hope to investigate this important question in future work.

With known value of $\Delta\omega$, the phonon mean free path $l(\omega)$ can be calculated as follows

$$l(\omega) = v_g \tau = \frac{v_g}{2\Delta\omega}. \quad (16)$$

The phonons are well defined excitations if their mean free path $l(\omega)$ exceeds the phonon wave length $\lambda = 2\pi/q$ (Ioffe-Regel criterium for phonons). As we will see in the next Section, phonons transform to diffusons when $l(\omega) \approx \lambda/2$. We will call the corresponding crossover frequency as ω_{IR} . Fig. 9 shows the ratio $l(\omega)/\lambda$ as a function of ω for several values of μ and different directions of the wave vector \mathbf{q} . The boundary between filled and open symbols (the full horizontal line) corresponds to frequency ω_{IR} . Thus filled and open symbols on Figs. 4, 7, 8, 9 belong to phonons with frequencies below and above the Ioffe-Regel crossover frequency correspondingly.

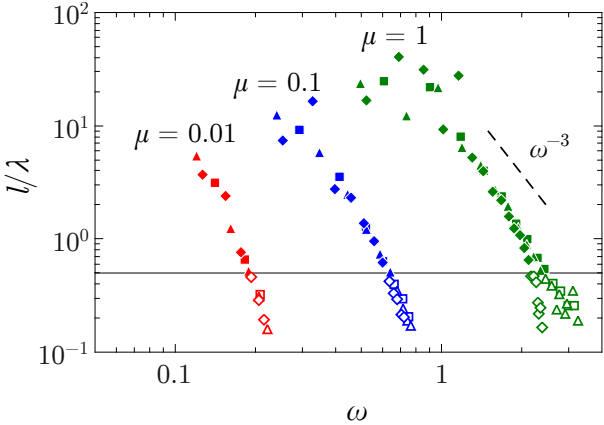


FIG. 9: The ratio $l(\omega)/\lambda$ as a function of ω for different μ . Different symbols correspond to different \mathbf{q} directions as explained on Fig. 8. The full horizontal line (separating filled and open symbols) corresponds to Ioffe-Regel crossover $l(\omega) = \lambda/2$.

Usually in glasses the Ioffe-Regel crossover frequency ω_{IR} is correlated with position of the boson peak ω_b , see⁴³⁻⁴⁶ and references therein. It is the frequency where the reduced DOS $g(\omega)/\omega^2$ has a maximum. We also have a rather sharp boson peak in our disordered lattices³⁴.

As is evident from Fig. 4, it comes from vibrations in the low frequency range of the dynamical matrix $M = AA^T$. These vibrations are pushed out to higher frequencies when we add to the dynamical matrix AA^T a crystalline part μM_0 . Just these vibrations, forming an additional density of states near frequency ω_{\max} , are responsible for the boson peak in our case. As follows from Fig. 4 the left side of the boson peak is constructed from phonons having negative dispersion $\omega_{\mathbf{q}}$. Similar results were obtained recently for Lennard-Jones glasses^{42,47,48}. It is not inconceivable that the boson peak in some other glasses can have a similar structure.

The frequencies ω_{\max} , ω_{IR} , and ω_b are collected in Table I for different μ . As we can see from the table, ω_{IR} is close to the frequency ω_{\max} and to the position of the boson peak ω_b . Above ω_{IR} phonons cease to exist as well defined excitations. They are smoothly transformed to diffusons which we will consider in the next Section. The relative number of phonons in the lattice can be estimated as follows

$$N_{\text{ph}} = \int_0^{\omega_{\text{IR}}} g(\omega) d\omega. \quad (17)$$

These values are also given in the Table I. We see that for all investigated values of μ the relative number of phonons in the lattice is small. It is in agreement with similar estimates for amorphous silicon²⁶.

μ	ω_{\max}	ω_b	ω_{IR}	N_{ph}
1	2.5	2.4	2.2*	0.12
0.1	0.78	0.74	0.62	0.027
0.01	0.23	0.23	0.19	0.0066
0.001	0.072	0.07		

TABLE I: The frequency of maximum in DOS ω_{\max} , the frequency of the Ioffe-Regel crossover ω_{IR} and the boson peak frequency ω_b for various μ . Star * means that ω_{IR} was found for $\mathbf{q} \parallel \langle 100 \rangle$ direction. N_{ph} is a relative number of phonons in the lattice.

IV. DIFFUSONS

In this section we are going to consider properties of diffusons. As is well known, the diffusion phenomenon usually takes place for physical quantities which are conserved. In a free closed mechanical system we have two integrals of motion, momentum and energy.

A. Diffusion of momentum

First let us consider diffusion of momentum. Usually the diffusion of momentum is related to viscosity in the system. All particle masses being equal ($m_i = 1$), the diffusion of momentum is equivalent to the diffusion of

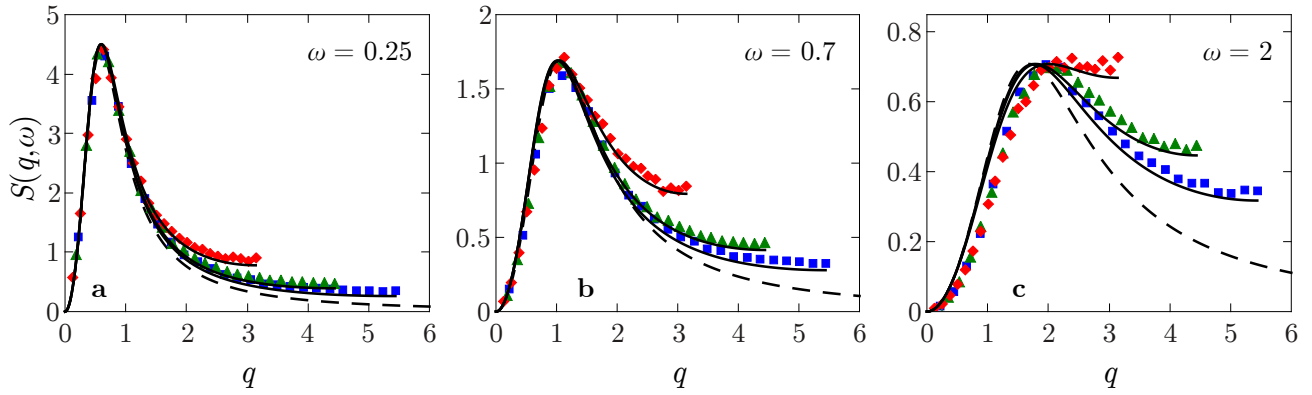


FIG. 10: The displacement structure factor $S(\mathbf{q}, \omega)$, Eq. (11) (symbols) for $\mu = 0$ and for three different frequencies. The sample size is $N = 50^3$. The averaging is performed over 300 realizations. Different symbols correspond to different \mathbf{q} directions. \diamond for $\mathbf{q} \parallel \langle 100 \rangle$, \triangle for $\mathbf{q} \parallel \langle 110 \rangle$, \square for $\mathbf{q} \parallel \langle 111 \rangle$. Full lines correspond to the structure factor $S_{\text{rw}}(\mathbf{q}, \omega)$ of the random walk on the lattice given by Eq. (19) with $D_{\text{rw}} = 0.7$. Dashed line corresponds to the limit $q \ll 1$ (see Eq. (22)).

particle displacements. It is because in our system the position of the center of inertia is conserved and we can put it at the origin of the coordinate system. Then the sum of all particle displacements vanishes

$$\sum_i u_i(t) = 0, \quad (18)$$

i.e. it is an integral of motion. The diffusion of displacements in this case looks like a diffusion of "particles" in a lattice where the total number of particles is conserved.

By analogy with diffusion of "particles" the information about diffusivity of displacements is absorbed in the displacement structure factor $S(\mathbf{q}, \omega)$ (11). We remind that to calculate this structure factor we ascribed at the initial moment $t = 0$ the random displacements to all the particles with Gaussian distribution (with zero mean and unit variance) and velocities equal to zero. So the condition (18) at $t = 0$ was satisfied. Therefore let us analyze now this structure factor in the diffuson frequency range.

Consider first the case of $\mu = 0$ when phonons are absent and only diffusons are present in the lattice. Fig. 10 shows the structure factor $S(\mathbf{q}, \omega)$ as a function of wave vector q for three different directions in \mathbf{q} space (symbols) and for three different frequencies ω . Let us compare this displacement structure factor with structure factor of the random walk $S_{\text{rw}}(\mathbf{q}, \omega)$ on the lattice.

As was shown in⁴⁹ for the case of the random walk on a lattice, $S_{\text{rw}}(\mathbf{q}, \omega)$ is given by expression

$$S_{\text{rw}}(\mathbf{q}, \omega) = \frac{2\Gamma(\mathbf{q})}{\omega^2 + \Gamma^2(\mathbf{q})}. \quad (19)$$

It is a Lorentzian, with a width $\Gamma(\mathbf{q})$ given by

$$\Gamma(\mathbf{q}) = D_{\text{rw}}Q^2(\mathbf{q}), \quad (20)$$

where D_{rw} is a diffusion constant of the random walk. In a simple cubic lattice (with lattice constant $a_0 = 1$) the function $Q(\mathbf{q})$ reads

$$Q(\mathbf{q}) = 2\sqrt{\sin^2 \frac{q_x}{2} + \sin^2 \frac{q_y}{2} + \sin^2 \frac{q_z}{2}}. \quad (21)$$

For small values of $q \ll 1$, $Q(\mathbf{q}) = q$ and in the continuum limit we have the well known result for the diffusion structure factor

$$S_{\text{rw}}(\mathbf{q}, \omega) = \frac{2D_{\text{rw}}q^2}{D_{\text{rw}}^2q^4 + \omega^2}. \quad (22)$$

Let us note that the structure factor (19) has a maximum at \mathbf{q} values obeying the condition

$$\omega = \Gamma(\mathbf{q}) = D_{\text{rw}}Q^2(\mathbf{q}). \quad (23)$$

We can specify it as a *dispersion law for diffusons*. The width of the maximum is $\Gamma(\mathbf{q})$. For $q \ll 1$, $\Gamma(\mathbf{q}) = D_{\text{rw}}q^2$.

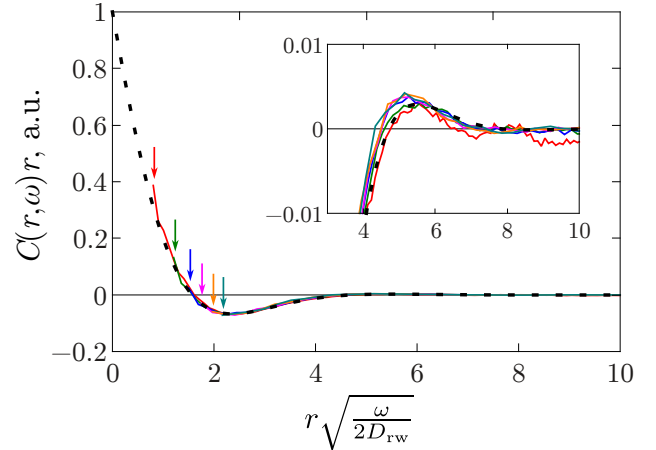


FIG. 11: The correlation function $C(\mathbf{r}, \omega)$ for $\mu = 0$ and six frequencies ω (0.14, 0.31, 0.49, 0.66, 0.84, 1.01) for sample with $N = 50^3$ particles averaged over 300 realizations. The full lines are our numerical results obtained from Eq. (11). Each line starts from $r = r_{\text{min}}$ which is about 2.5 interatomic distances (marked by arrows). The dashed line corresponds to Eq. (26) with $D_{\text{rw}} = 0.7$.

A comparison of the displacement structure factor $S(\mathbf{q}, \omega)$, (11), and the structure factor of the random

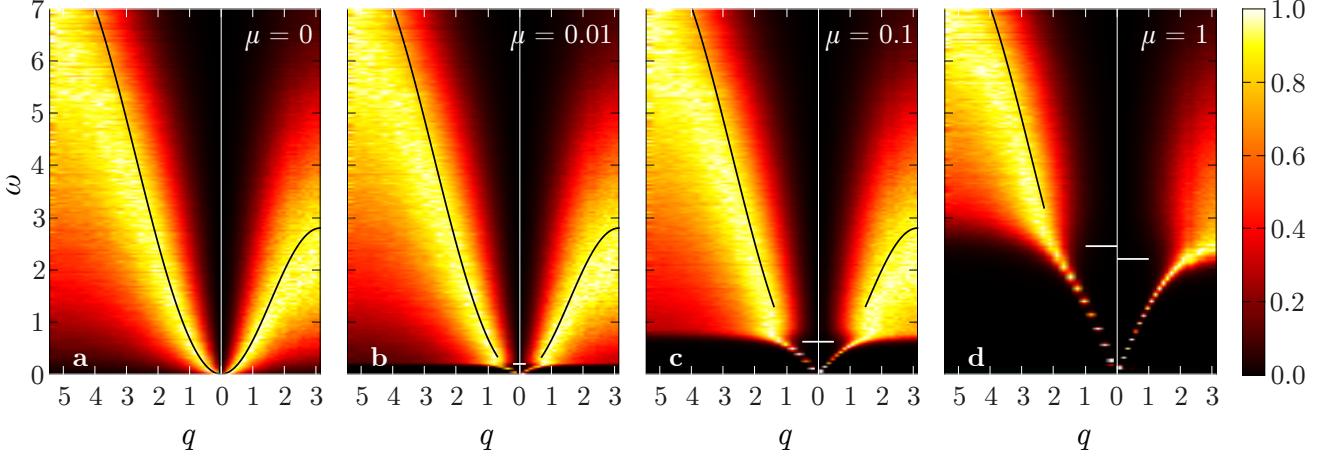


FIG. 12: The normalized structure factor $S_n(\mathbf{q}, \omega)$ as a function of q for some direction in \mathbf{q} space and for each frequency ω for various values of μ (0, 0.01, 0.1, 1). The sample size is $N = 50^3$. The averaging is performed over 100 realizations. Left sides of all plots are for $\mathbf{q} \parallel \langle 111 \rangle$, right sides are for $\mathbf{q} \parallel \langle 100 \rangle$. White horizontal dashes show the Ioffe-Regel crossover frequency ω_{IR} . For $\mu = 1$ the frequency ω_{IR} is slightly different for different \mathbf{q} directions. Black full line corresponds to Eq. (23) for the random walk on a simple cubic lattice with diffusion constant $D_{\text{rw}} = 0.7$.

walk $S_{\text{rw}}(\mathbf{q}, \omega)$, (19), is shown on Fig. 10. One fitting parameter was the diffusion coefficient D_{rw} in Eq. (20). From comparison of these data we obtained $D_{\text{rw}} \approx 0.7$. It means that the diffusion coefficient of particle displacements $D_u \approx 0.7$ (see Section V). Another fitting parameter was a height $h(\omega)$ of the random walk structure factor in the maximum. According to Eq. (19), in the maximum $\Gamma(\mathbf{q}) = \omega$ and $h(\omega) = 1/\omega$, but to fit the data points on Fig. 10 we used slightly higher values of $h(\omega)$.

The small difference between $h(\omega)$ and $1/\omega$ can be explained by different frequency dependencies of the density of states $g(\omega)$ for vibrations and for the random walk (following from the sum rule similar to Eq. (13)). As we can see from the figure, for the investigated frequencies the fit is perfect. With increasing frequency above $\omega \approx 2 - 3$, the fitting becomes more and more poor since we approach the localization threshold at $\omega_{\text{loc}} \approx 5.5 \pm 0.5$ (see below) which is not described well by a simple model of Markovian random walk.

Now let us consider a behavior of a correlation function. The correlation function of particle displacements at some frequency ω , expressed through eigenvectors $e_{\mathbf{r}}(\omega)$ of the dynamical matrix M , reads

$$C(\mathbf{r}, \omega) = \sum_{\mathbf{r}'} e_{\mathbf{r}'+\mathbf{r}}(\omega) e_{\mathbf{r}'}(\omega). \quad (24)$$

It is a Fourier transform of the displacement structure factor (11)

$$C(\mathbf{r}, \omega) = \frac{1}{8\pi^4} \int S(\mathbf{q}, \omega) e^{i\mathbf{q}\mathbf{r}} d\mathbf{q}. \quad (25)$$

Let us compare this correlation function with correlation function of the random walk. For distances bigger than the period of the lattice ($a_0 = 1$) we can make use of the limit of small $q \ll 1$ and integrate Eq. (22) for the

random walk structure factor taken in approximation of continuous media. As a result, we derive

$$C_{\text{rw}}(\mathbf{r}, \omega) = \frac{\exp\left(-r\sqrt{\frac{\omega}{2D_{\text{rw}}}}\right) \cos\left(r\sqrt{\frac{\omega}{2D_{\text{rw}}}}\right)}{2\pi^2 r D_{\text{rw}}}. \quad (26)$$

Fig. 11 shows a good agreement of our correlation function (25) with the correlation function of the random walk (26). For all investigated frequencies the numerical data collapse together and become indistinguishable from the theoretical prediction (26). We can see also on this figure the anticorrelation phenomenon (the region of negative values of the correlation function). As follows from Eq. (26), the correlation function of the random walk changes its sign for the first time at

$$r\sqrt{\frac{\omega}{2D_{\text{rw}}}} = \frac{\pi}{2}. \quad (27)$$

It is also in a good agreement with our numerical results. Therefore we can call a corresponding value of r found from Eq. (27) as a *radius of diffuson*. It is a typical size of the regions vibrating with frequency ω and having the same sign of all particle displacements.

Now let us analyze the displacement structure factor $S(\mathbf{q}, \omega)$ for $\mu \neq 0$. For better visual effect we will show a map of the function $S(\mathbf{q}, \omega)$ on the plane (ω, q) for different directions in \mathbf{q} space. To do that, for each frequency ω we have found the maximum $S(\mathbf{q}, \omega)$ as a function of q along some directions in \mathbf{q} space. Then we normalized function $S(\mathbf{q}, \omega)$ along this line $\omega=\text{const}$ to the magnitude of this maximum.

The results are shown on Fig. 12 for four different values of μ and two directions in \mathbf{q} space. The white color corresponds to the maximum when normalized structure factor $S_n(\mathbf{q}, \omega) = 1$ while the black color to the case

where $S_n(\mathbf{q}, \omega) = 0$. For $\mu \neq 0$ we can see clearly two types of excitations in the lattice. At low enough frequencies, below ω_{IR} , we see phonons with well defined dispersion law $\omega_{\mathbf{q}}$, the same as in the previous Section. At the Ioffe-Regel crossover frequency ω_{IR} , the structure factor strongly broadens and phonon dispersion line disappears. Above ω_{IR} the displacement structure factor coincides well with the structure factor for $\mu = 0$ case shown on Fig. 12a, which corresponds to diffusons. The maximum of the normalized structure factor $S_n(\mathbf{q}, \omega)$ (white regions) agrees well with Eq. (23) giving the maximum of the random walk structure factor $S_{\text{rw}}(\mathbf{q}, \omega)$ (black line). Deviations from $S_{\text{rw}}(\mathbf{q}, \omega)$ take place at high frequencies near the localization threshold.

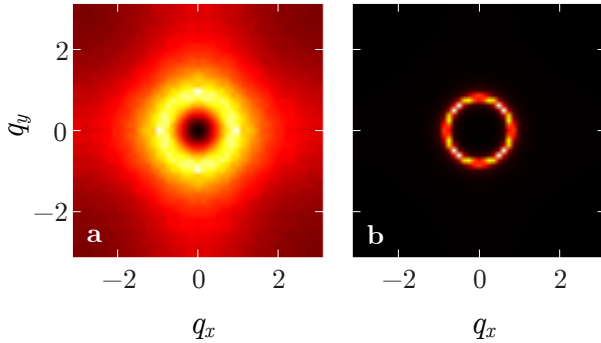


FIG. 13: The same normalized structure factor $S_n(\mathbf{q}, \omega)$ as on Fig. 12 but in \mathbf{q} space in plane $q_x q_y$ ($q_z = 0$) for $\omega = 0.5$. The left picture corresponds to $\mu = 0$ (a) and the right to $\mu = 0.1$ (b).

Finally, to compare phonon and diffuson structure factors, a cross section of the structure factor $S_n(\mathbf{q}, \omega)$ in \mathbf{q} space for $q_z = 0$ and frequency $\omega = 0.5$ is shown on Fig. 13 for $\mu = 0$ and $\mu = 0.1$. At the left side (a) of this figure we see the structure factor of diffuson. On the right side we see the structure factor of phonon (b). As compared with phonon structure factor, the diffuson structure factor is much more broadened.

B. Diffusion of energy

Now let us consider the diffusion of energy. The diffusion of energy is different from diffusion of particle displacements (see Section V). The first approach to calculate the diffusivity of energy $D(\omega)$ for vibrations with frequency ω is a direct numerical solution of Newton's equations. For that we have used the Runge-Kutta-4 method with time step $\Delta t = 0.01$ applied to a cubic sample with $N = L \times L \times L$ particles (lattice constant $a_0 = 1$) and with free boundary conditions along the x direction. Along other two directions we take the periodic boundary conditions.

Assuming zero initial conditions for displacements and velocities of all the particles, let us apply external forces with frequency ω and random phases φ_i to the particles

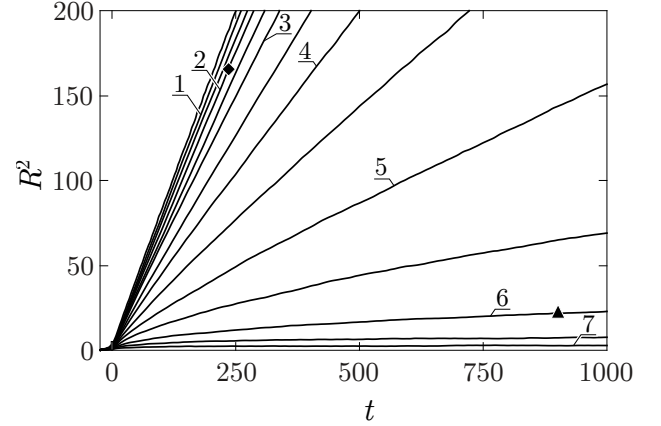


FIG. 14: The dependence of $R^2(t)$ in the case of $\mu = 0$ for one sample with $N = 100 \times 100 \times 100$ particles and 14 different frequencies $\omega = 0.5, 1, 1.5, \dots, 7$ (from top to bottom). The numbers indicate integer frequencies. The slope of each line corresponds to each black dot in Fig. 15. Two points at $\omega = 2$ and $\omega = 6$ correspond to two distributions of energy $E(x, t)$ over the sample for delocalized and localized modes correspondingly. They are shown on Fig. 16 (see below).

in the central layer $x = 0$ of our sample

$$f_i^{\text{ext}}(t) = \sin(\omega t + \varphi_i) \exp\left(-\frac{t^2}{2T^2}\right) \quad (28)$$

where $\omega T \gg 1$. The right and the left sides of the sample have coordinates $x_{\text{r,l}} = \pm L/2$. In such a way we excite vibrations with frequencies near frequency ω distributed in a small frequency interval $(\omega - 1/T, \omega + 1/T)$. In calculations we used $T = 5$ for all frequencies ω . We started our calculations at time $t_0 = -5T$ when the external force is still negligible.

After applying the force to the central layer $x = 0$, vibrations will spread to the left and to the right ends of the sample. The average squared distance to the energy diffusion front we define as usual

$$R^2(t) = \frac{1}{E_{\text{tot}}} \sum_{i=1}^N x_i^2 E_i(t) = \frac{1}{E_{\text{tot}}} \int_{-L/2}^{L/2} x^2 E(x, t) dx. \quad (29)$$

Here x_i is the x coordinate of the i -th particle, $E_i(t)$ is the energy of i -th particle and sum is taken over all particles in the sample. $E_{\text{tot}} = \sum_i E_i(t)$ is the total energy of the system. It is independent of time after the external force $f_i^{\text{ext}}(t)$ becomes negligibly small (i.e. for $t > 5T$).

The energy of i -th particle $E_i(t)$ we define as a sum of the kinetic energy and a half of the potential energy of connected bonds ($m_i = 1$)

$$E_i(t) = \frac{v_i(t)^2}{2} - \frac{1}{4} \sum_j M_{ij} (u_i(t) - u_j(t))^2. \quad (30)$$

Here $v_i(t) = \dot{u}_i(t)$ is a particle velocity. Summation over all particles in Eq. (29) we can divide in two steps. First

we sum over all particles in the layer x and then we sum over all layers. Let $E(x, t)$ be a total energy confined to the layer x at time t . Having in mind that in our case we have lattice constant $a_0 = 1$ and sample size $L \gg 1$, we can change summation over different layers to integration over coordinate x for times where $R(t) \gg 1$.

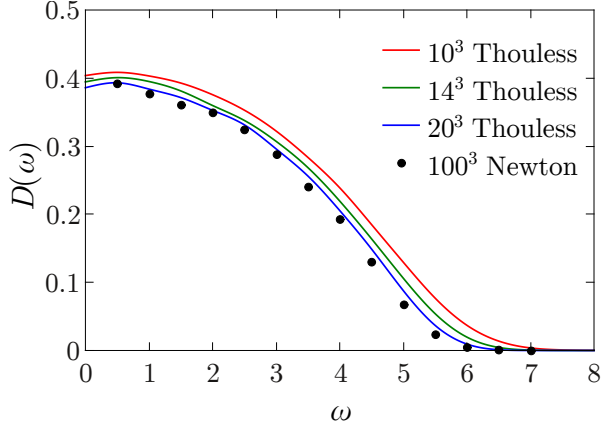


FIG. 15: The dependence of diffusivity $D(\omega)$ on ω for $\mu = 0$. Black dots are calculated by the direct solution of Newton's equations from Eqs. (29, 31) and Fig. 14 for $N = 100^3$ particles (one realization). Full lines for $N = 10^3, 14^3, 20^3$ are calculated using formula of Edwards and Thouless (36) with $c = 1$ (see below). Averaging for lines is performed over frequencies in the small interval $(\omega - \delta\omega, \omega + \delta\omega)$ with $\delta\omega = 0.25$ and over several thousands realizations.

We will apply this method to the case of $\mu = 0$ (i.e. for the lattice without phonons). The results are shown on Fig. 14. As we can see from the figure for small and middle frequencies, $R^2(t) \propto t$. Therefore for these frequencies vibrations indeed spread along the x axis by means of diffusion. The slope of the lines decreases with frequency ω . For calculating the slope, we take the time interval Δt where, on the one hand $t > 5T$, and on the other hand, $R \ll L/2$.

From the slope of $R^2(t)$ we can calculate the diffusivity of modes $D(\omega)$ using one dimensional formula

$$R^2(t) = 2D(\omega)t. \quad (31)$$

This diffusivity is shown by black dots on Fig. 15. At small frequencies it is approximately constant, then it decreases with frequency approaching zero at the localization threshold, $\omega_{\text{loc}} \approx 5.5 \pm 0.5$. At higher frequencies above ω_{loc} the dependence $R^2(t)$ saturates with increasing t . This indicates localization of the vibrational modes.

The difference between delocalized and localized modes is clearly seen if we examine the dependence $E(x, t)$ as a function of coordinate x at some moment t for two different frequencies below and above the localization threshold. These two points for investigation are shown on Fig. 14. Black diamond corresponds to delocalized mode with frequency $\omega = 2$ and has coordinates $t = 234$ and $R^2 = 166$. The distribution of energy $E(x, t)$ over the

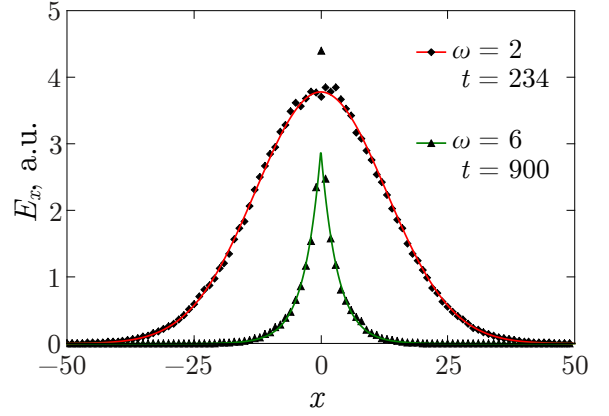


FIG. 16: Black points (diamonds and triangles) show the distribution of energy $E(x, t)$ contained in the layer x as a function of x for two different frequencies $\omega = 2$ and $\omega = 6$ at times $t = 234$ and $t = 900$, respectively, calculated numerically with Newton method. Full lines are theoretical predictions for delocalized (diffusive) and localized modes given by Eqs. (32, 33) with $R^2 \approx 166$ and $R^2 \approx 22$ correspondingly.

sample calculated numerically at this moment is shown by black diamonds on Fig. 16. The data are perfectly fitted by solid line drawn according to the solution of diffusion equation in 1d case

$$E(x, t) = \frac{E_{\text{tot}}}{\sqrt{2\pi R^2}} \exp\left(-\frac{x^2}{2R^2}\right), \quad (32)$$

with value of $R^2 = 166$.

Black triangle on Fig. 14 corresponds to localized mode with frequency $\omega = 6$ and has coordinates $t = 900$ and $R^2 = 22$. The distribution of energy $E(x, t)$ over the sample calculated numerically at this moment is shown by black triangles on Fig. 16. This distribution is drastically different from the previous case. For localized modes we expect the usual exponential decay

$$E(x, t) = \frac{E_{\text{tot}}}{\sqrt{2}R} \exp\left(-\frac{\sqrt{2}|x|}{R}\right). \quad (33)$$

The fit of the numerical data with this function and $R^2 = 22$ is shown on Fig. 16. The fit is perfect except for the central point at $x = 0$ which lies noticeably above prediction of Eq. (33). The coefficients in Eqs. (32, 33) were taken to satisfy the obvious rules

$$\int_{-\infty}^{\infty} E(x, t) dx = E_{\text{tot}}, \quad \frac{1}{E_{\text{tot}}} \int_{-\infty}^{\infty} x^2 E(x, t) dx = R^2. \quad (34)$$

To find the diffusivity $D(\omega)$ for $\mu \neq 0$, the method of numerical solution of Newton's equations is not appropriate, because in this case we have phonons in the lattice with long mean free paths. Correspondingly samples with much bigger sizes are necessary to use this approach. Therefore for $\mu \neq 0$ we used a second approach.

In this approach, the diffusivity $D(\omega_i)$ at eigenfrequency ω_i was calculated by means of the formula of Edwards and Thouless⁵⁰

$$D(\omega_i) \simeq L^2 |\Delta\omega_i| \quad (35)$$

where L is the length of the sample and $\Delta\omega_i$ is sensitivity of the eigenfrequency ω_i to a twist of boundary conditions. More precisely, we defined the diffusivity as follows:

$$D(\omega) = c \lim_{\varphi \rightarrow 0} \frac{L^2}{\varphi^2} \langle |\Delta\omega(\omega)| \rangle \quad (36)$$

where φ is the angle of twisting, and c is some constant of the order of unity. It will be determined from comparison with the Newton method. The averaging in Eq. 36 is performed over frequencies ω in the small interval $(\omega - \delta\omega, \omega + \delta\omega)$ with $\delta\omega = 0.25$ and/or over several thousands realizations.

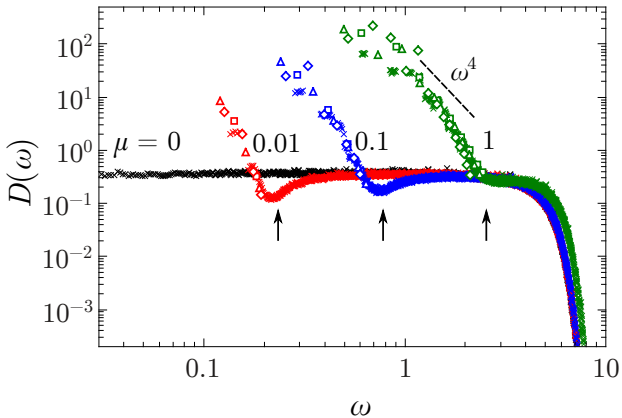


FIG. 17: The diffusivity $D(\omega)$ for various μ (0, 0.01, 0.1, 1) for sample with $N = 14^3$ (crosses). The diffusivity was calculated using formula of Edwards and Thouless (36) with $c = 1$ and averaged over two thousand realizations. The arrows indicate frequencies ω_{\max} in the DOS $g(\omega)$ for corresponding values of μ . Open symbols correspond to phonon diffusivity (39) below the Ioffe-Regel crossover frequency ω_{IR} .

The symmetric real matrix M was defined as usual (5) with periodic boundary conditions. The twisting of the matrix M by angle φ gives a new Hermitian matrix M' obtained as follows. For bonds between the left (l) and the right (r) boundaries of our cubic sample

$$M'_{lr} = M_{lr} \exp(i\varphi), \quad M'_{rl} = M_{rl} \exp(-i\varphi). \quad (37)$$

For all other bonds $M'_{jk} = M_{jk}$. So $\Delta\omega_i$ is the difference between i -th eigenfrequencies of matrices M and M'

$$\Delta\omega_i = \omega_i - \omega'_i. \quad (38)$$

Twisting of boundary conditions was performed for x direction only. For others two directions the periodic boundary conditions were used.

For $\mu = 0$ the results for $D(\omega)$ are shown on Fig. 15 for three different cubic samples (full lines). We compared these results with numerical solution of Newton equations for $\mu = 0$ (black dots) and get for the constant $c \approx 1$. Then we used this c value for $\mu \neq 0$. The results are shown on Fig. 17. For $\mu \neq 0$ we see clearly two different frequency regions in the function $D(\omega)$.

At low frequencies, diffusivity increases with decreasing of ω . This range corresponds to the phonons. Indeed, the diffusivity of phonons $D(\omega)$ can be calculated as follows

$$D(\omega) = \frac{1}{3} l(\omega) v_g(\omega). \quad (39)$$

Open symbols on Fig. 17 show contribution calculated from this equation (just below Ioffe-Regel threshold). We see a good agreement with Edwards and Thouless formula. After a deep minimum at frequency $\omega \approx \omega_{\max}$ the diffusivity $D(\omega)$ saturates at a constant level coinciding with $D(\omega)$ for $\mu = 0$. The diffusivity in this range corresponds to diffusons. Similar behavior of $D(\omega)$ was found in jammed systems^{31,32}. The deep minimum in the diffusivity at $\omega \approx \omega_{\max}$ corresponds to strong scattering of phonons by the quasilocal vibrations near the sharp peaks in the DOS $g(\omega)$ (see Fig. 4).

V. DISCUSSION

We have developed a random matrix approach to describe vibrations in strongly disordered systems, which have properties similar to what one observes in granular matter at the jamming transition point, in jammed systems and, finally, in real glasses. This approach has one important advantage in comparison to other models. It describes mechanical systems which are always stable independently of the degree of disorder. Previous random matrix models^{13,40,51} suffer from an inherent mechanical instability that occurs at some critical amount of disorder. As a result, they are limited by consideration of "relatively weak" or "moderate" disorder.

We take the dynamical matrix in the form $M = AA^T + \mu M_0$. Here A is a random matrix $N \times N$ built on a simple cubic lattice with N particles and interaction between nearest neighbors only. The only non zero non-diagonal matrix elements A_{ij} between the nearest neighbors are taken as independent random numbers from Gaussian distribution with zero mean $\langle A_{ij} \rangle = 0$ and unit variance $\langle A_{ij}^2 \rangle = 1$. The variance controls the degree of disorder in the lattice. To ensure the translational invariance the diagonal elements are calculated as a minus sum of non-diagonal elements $A_{ii} = -\sum_{j \neq i} A_{ji}$. M_0 is a simple crystalline dynamical matrix with unit springs between the nearest neighbors.

If the first term AA^T is responsible for the disorder in the system, the second term μM_0 describes the ordered part of the Hamiltonian. The parameter μ controls the relative amplitude of this part and the rigidity of the

lattice. It can vary in the interval $0 \leq \mu < \infty$, changing the rigidity and relative amount of disorder. In this paper we have mainly considered the case of strong disorder when $0 \leq \mu \leq 1$ and fluctuating part of the dynamical matrix is bigger than the ordered part. In this case the Young modulus of the lattice $E \propto \sqrt{\mu}$. Such form of the dynamical matrix guarantees the mechanical stability of the system for any positive value of μ .

We have found that the delocalized vibrational excitations in this disordered lattice are of two types. At low frequencies below the Ioffe-Regel crossover, $\omega < \omega_{\text{IR}}$, they are the usual phonons (plane waves) which can be characterized by frequency ω and wave vector \mathbf{q} . However, with increasing of ω , due to the disorder-induced scattering, the phonon line width $\Delta\omega$ increases rapidly as $\Delta\omega \propto \omega^4$ and at some frequency $\omega \approx \omega_{\text{IR}}$ the phonon mean free path l becomes of the order of the wave length λ . Though this crossover is not sharp and has no critical behavior at $\omega = \omega_{\text{IR}}$, the structure of the eigenmodes at higher frequencies quite soon become very different from the plane waves.

As a result, at higher frequencies the original notion of phonons is lost and delocalized vibrational modes have a diffusive nature. They are similar to *diffusons* introduced by Allen and Feldman, et al.²⁶. The diffusons again can be characterized by frequency ω , but have no well defined wave vector \mathbf{q} . Above $\omega \approx \omega_{\text{IR}}$ the structure factor of particle displacements $S(\mathbf{q}, \omega)$ becomes very similar to the structure factor $S_{\text{rw}}(\mathbf{q}, \omega)$ of a random walk on the lattice. The former has a broad maximum as a function of q at $q = \sqrt{\omega/D_u}$, where D_u is a diffusion coefficient of the particle displacements.

The displacement structure factor $S(q, t)$ in the diffuson range, for small $q \ll 1/a_0$, decays as following, $S(q, t) \propto \exp(-D_u q^2 t)$. As a result the vibrational line width $\Gamma(q) = D_u q^2$. Such quadratic dependence of $\Gamma(q)$ was found in many glasses in the experiments on inelastic x-ray scattering, see for example^{52,53} and references therein. It was also found in molecular dynamic simulation of amorphous silicon⁵⁴. However in these and other papers this line width was attributed to phonons without discussion of its physical origin. We guess that the observed q^2 dependence of $\Gamma(q)$ has nothing to do with phonons and is in fact related to diffusons. However, a more detailed investigation is necessary for a definite conclusion.

The crossover between phonons and diffusons takes place at the Ioffe-Regel crossover frequency ω_{IR} which is close to the position of the boson peak. Since for phonons $\Delta\omega \propto \omega^4$ and for diffusons $\Gamma(q) = D_u q^2$, there should exist a crossover from ω^4 to q^2 dependence of the line width. Such a crossover was indeed found recently in inelastic x-ray scattering in lithium diborate glass⁴⁵, densified vitreous silica⁵⁵, vitreous silica⁵⁶⁻⁵⁸, glassy sorbitol⁵⁹ and glycerol glass⁶⁰. The crossover frequency was found to be close to the BP position.

As a result, if our guess is true, we can calculate the diffusion coefficient of particle displacements, $D_u =$

$\Gamma(q)/q^2$, from the experimental line width $\Gamma(q)$ in the range, where it is proportional to q^2 . Taking into account that $D_u \approx a_0^2/\tau$ where a_0 is the lattice constant and τ is an average time for a jump, we come to the order of the value estimate $D_u \approx 1 \text{ mm}^2/\text{sec}$ for $a_0 \approx 2 \text{ \AA}$ and $\tau \approx 0.4 \times 10^{-13} \text{ sec}$. Let us compare this value with experimental data.

In the paper⁵⁷ it was found that in vitreous silica $\hbar\Gamma/(\hbar\omega)^2 = 0.07 \text{ meV}^{-1}$ for $q \geq 2 \text{ nm}^{-1}$. Taking the sound velocity $v_L = 5250 \text{ m sec}^{-1}$ for $q = 2 \text{ nm}^{-1}$ we get for diffusion coefficient $D_u = 1.3 \text{ mm}^2/\text{sec}$. Let us compare this value with the diffusivity of energy $D(\omega)$ for small ω in the same glass. We expect that both coefficients should be of the same order of magnitude. The diffusivity of energy $D(\omega)$ in vitreous silica was calculated in the paper²⁹. It was obtained that $D(0) = 1.4 \text{ mm}^2/\text{sec}$. A close estimate $D(0) = 1.1 \text{ mm}^2/\text{sec}$ was given in³⁰. As one can see the agreement between D_u and $D(0)$ is unexpectedly good. In glycerol glass⁶¹ we found the diffusivity about factor of two smaller, $D_u = 0.46 \text{ mm}^2/\text{sec}$. For amorphous silicon from molecular dynamic calculations⁵⁴ we get $D_{ul} = 3.2 \text{ mm}^2/\text{sec}$ for longitudinal vibrations, and $D_{ut} = 1.2 \text{ mm}^2/\text{sec}$ for transverse vibrations. For the diffusivity of energy we have in this glass the estimate²⁶ $D(0) = 0.6 \text{ mm}^2/\text{sec}$.

Since $\omega_{\text{IR}} \propto \sqrt{\mu}$, we can vary the Ioffe-Regel crossover frequency and, therefore, the relative number of phonons N_{ph} in the system, changing the parameter μ . It is zero when $\mu = 0$ and there are no phonons in the lattice. In this case all delocalized vibrations are diffusons. If $0 < \mu \ll 1$ we have phonons, but their relative number is small. One can show that in this case $N_{\text{ph}} \propto \mu^{3/4}$. In the opposite case, $\mu \gg 1$, the disorder is relatively small and nearly all vibrations in the lattice are well defined plane waves, i.e. phonons.

In amorphous silicon the relative number of phonons (plane waves) was estimated to be only 4% from all of the vibrational modes in the system²⁶. The estimates show that in our model we have such a small amount of propagating modes, as in a-Si, for $\mu \approx 0.1$. In the silica glass we can estimate the relative number of phonons from the data¹¹. Taking into account that Ioffe-Regel crossover frequency in amorphous silica was estimated to be¹¹ $\nu_{\text{IR}} = 1 \text{ THz}$, and integrating density of states¹¹ up to this frequency we come to the relative number $N_{\text{ph}} = 0.002 \pm 0.0005$. As a result in the typical glass such as amorphous silica only 0.2 % of all modes are phonons. As follows from Table I it corresponds to very small values of $\mu < 0.01$. It means that small amount of phonons in disordered systems is a signature of strong disorder.

Usually the phenomenon of diffusion takes place for conserved quantities. In our system we have two integrals of motion. They are the momentum and the energy of the lattice. Therefore, first of all, one has to discriminate the diffusion of particle momentums (or particle displacements) from the diffusion of energy. Conservation of displacement is related to conservation of the center of inertia in the system. As a result, the diffusion of par-

ticle displacements has the same diffusion coefficient as the diffusion of particle momentums.

The diffusion coefficient of displacements/momentums $D_{u/v}$ is hidden in the displacement structure factor $S(\mathbf{q}, \omega)$ (11). Comparing this structure factor with the structure factor of the random walk on the lattice, we found that for the case of $\mu = 0$ the diffusion coefficient $D_{u/v} = D_{rw} = 0.7$. We can check that it is indeed the diffusion coefficient of particle displacements/momentums in a similar way we used for finding the diffusivity of energy $D(\omega)$ in Section IV B.

Let us consider a cubic random lattice $L \times L \times L$ with $\mu = 0$ and unit masses $m_i = 1$ with periodic boundary conditions. At initial moment $t = 0$ let us displace all particles in a thin layer around the central layer (with coordinate $x = 0$) according to Gaussian distribution

$$u(x, 0) = u_0 e^{-x^2/2x_0^2}. \quad (40)$$

Here the thickness of the layer x_0 should be small enough in comparison to the sample size L , i.e. $x_0 \ll L/2$. Initial velocities $\dot{u}(0)$ of all the particles are equal to zero.

After initial displacements in the thin central layer, the particle displacements will diffuse to the left and to the right ends of the sample. Solving numerically the Newton equations, we find the average squared distance to the displacement diffusion front, similar to Eq. (29)

$$R_u^2(t) = \frac{1}{u_{\text{tot}}} \sum_i x_i^2 u_i(t), \quad u_{\text{tot}} = \sum_i u_i(t). \quad (41)$$

Since the center of inertia does not move, the total displacement of all particles u_{tot} is independent of time and equal to the total displacement at $t = 0$.

From the slope of $R_u^2(t)$ we can calculate the diffusion coefficient of the displacements D_u as follows

$$R_u^2(t) = 2D_u t \quad (42)$$

similar to Eq. (31).

In the same way we can calculate the diffusion of momentum. For that at the moment $t = 0$ initial displacements of all the particles we put equal to zero. However initial velocities $v = \dot{u}(0)$ in the thin central layer we take distributed similar to Eq. (40)

$$v(x) = v_0 e^{-x^2/2x_0^2}. \quad (43)$$

Then, as in the previous case, solving numerically the Newton equations we find

$$R_v^2(t) = \frac{1}{v_{\text{tot}}} \sum_i x_i^2 v_i(t), \quad v_{\text{tot}} = \sum_i v_i(t). \quad (44)$$

Since the total momentum is conserved, v_{tot} is also independent of time and equal to its initial value at $t = 0$. From the slope of $R_v^2(t)$ we can calculate the diffusion coefficient of the momentum D_v using one dimensional equation

$$R_v^2(t) = 2D_v t \quad (45)$$

similar to Eq. (42).

In both cases we have obtained for diffusion coefficients D_u and D_v the same value as was derived from the structure factor, $D_u \approx D_v \approx D_{rw} = 0.7$. It confirms our statement that the displacement structure factor $S(\mathbf{q}, \omega)$ gives us the information about diffusion of particle displacements (or momentums). The diffusion of momentum is usually related to viscosity η of the medium. Therefore in the case of $\mu = 0$ our lattice has no rigidity but has a finite value of viscosity.

In disordered lattices the diffusion of energy is different from the diffusion of particle displacements (momentums). In the harmonic approximation the eigenmodes with different frequencies do not interact with each other. Therefore the energy cannot be transferred from one eigenmode to other eigenmodes. It means that energy of every eigenmode $E(\omega_i)$ is conserved (with time). The total energy E_{tot} is just a sum of these eigenmode contributions

$$E_{\text{tot}} = \sum_i E(\omega_i). \quad (46)$$

As a result, instead of one integral of motion (the total energy E_{tot}), in a scalar harmonic system with N particles we have N integrals of motion $E(\omega_i)$. And for each frequency ω_i we have its own unique energy diffusivity $D(\omega_i)$. At this point our model decidedly confirms the physical picture suggested in papers²²⁻²⁶ for amorphous silicon. We believe that it can be applied to some other glasses as well.

Usually this diffusivity is hidden in a displacement/momentums structure factor of the 4-th order. However, we calculated the diffusivity of energy $D(\omega)$ in a different way using two different approaches as it was discussed in Section IV B. The first approach is based on the direct solution of Newton equations. In the second approach we calculated the diffusivity using Edwards and Thouless formula⁵⁰. Both approaches give the same result.

In the first approach we used a short external force pulse Δt exciting vibrations in a small space region of the lattice and in a small frequency interval $\Delta\omega \approx 1/\Delta t$ near frequency ω . Then on a time scale $t \gg \Delta t$ the energy diffused through the lattice. Using Newton equations of motion we calculated this diffusion directly. It was supposed that the interval $\Delta\omega$ is much bigger than the interlevel spacing $\delta\omega$ and therefore the former consists of many eigenmodes. In the thermodynamic limit $\delta\omega \propto 1/N \rightarrow 0$ if $N \rightarrow \infty$. Therefore in an infinite system we can take the interval $\Delta\omega$ arbitrary small. The energy diffusion coefficient $D(\omega)$ in this case is a function of frequency ω . Approaching the localization threshold ω_{loc} the diffusivity $D(\omega)$ should go to zero.

We applied this method for $\mu = 0$, when there are no phonons in the lattice. In this case we obtained for diffusivity at zero frequency $D(0) \approx 0.4$, i.e. the value about factor of two smaller than for diffusivity of displacements, D_u . However this approach is rather difficult to imple-

ment for computer simulations in the case when $\mu \neq 0$. In this case we have phonons in the lattice with long mean free paths. And samples with much bigger sizes are necessary.

Therefore, to calculate the diffusivity $D(\omega)$ for arbitrary value of μ (including the case of $\mu = 0$), we used another approach. In this approach Edwards and Thouless formula⁵⁰, $D(\omega_i) = cL^2|\Delta\omega_i|$, was used. It relates the diffusivity $D(\omega_i)$ with shift of the eigenfrequencies $\Delta\omega_i$ due to change of the boundary conditions in one direction. The proportionality coefficient c we found from the comparison with the Newton method for $\mu = 0$. In this case both methods result in the same frequency dependence of $D(\omega)$.

The diffusivity of vibrational modes $D(\omega)$ in disordered lattices is a very important quantity. It determines the thermal conductivity²³

$$\kappa(T) \propto \int_0^\infty d\omega g(\omega) D(\omega) C(\omega, T). \quad (47)$$

Here $g(\omega)$ is density of states and $C(\omega, T)$ is specific heat of harmonic oscillator

$$C(\omega, T) = \left(\frac{\hbar\omega}{T}\right)^2 \frac{e^{\hbar\omega/T}}{(e^{\hbar\omega/T} - 1)^2}. \quad (48)$$

Localized modes have $D(\omega_i) = 0$ and make no contribution to $\kappa(T)$.

If functions $g(\omega)$ and $D(\omega)$ are approximately constant in some frequency interval (the case that we have, for example, in our picture for $\omega > \omega_{\text{IR}}$), then we find from Eq. 47 that approximately $\kappa(T) \propto T$ in the correspond-

ing temperature range. It explains a quasi-linear temperature dependence of the thermal conductivity above the plateau observed in glasses⁶. With increasing frequency the functions $g(\omega)$ and $D(\omega)$ finally drop to zero and thermal conductivity saturates at some constant level independent of temperature. Thus the conception of diffusons gives clear explanation for the temperature dependence of the thermal conductivity of glasses and other disordered systems.

Summarizing, using a stable random matrix approach we have presented a consequent theory of vibrational properties in strongly disordered systems. In these systems a relative amount of phonons is small and almost all delocalized vibrations are diffusons. The diffusons play an important role and are responsible for the transport properties of glasses at higher temperatures. Presumably they are also accounted for the mysterious q^2 dependence of the vibrational line width $\Gamma(q)$ observed in many experiments on inelastic x-ray scattering in glasses. Therefore we think that it is necessary to take them into account in interpretation of experimental data.

VI. ACKNOWLEDGMENTS

We are very grateful to V. L. Gurevich and Anne Tangy for many stimulating discussions and gratefully acknowledge interesting discussions with B. Rufflé and E. Courtens as well. One of the authors (DAP) thanks the University Lyon 1 for hospitality. This work was supported by St. Petersburg Government (diploma project no. 2.4/29-06/143C), Dynasty Foundation, RF President Grant “Leading Scientific Schools” NSh-5442.2012.2 and Russian Ministry of Education and Science (contract N 14.740.11.0892).

¹ S. Hunklinger and A. K. Raychaudhuri in *Progress in Low Temperature Physics*, edited by D. F. Brewer (Elsevier, Amsterdam, 1986), Vol. IX, p. 267.

² W. A. Phillips, Rep. Prog. Phys. **50**, 1657 (1987).

³ R. C. Zeller and R. O. Pohl Phys. Rev. B **4**, 2029 (1971).

⁴ U. Buchenau, Yu. M. Galperin, V. L. Gurevich, D. A. Parshin, M. A. Ramos, and H. R. Schober, Phys. Rev. B **46**, 2798 (1992).

⁵ D. A. Parshin, Sov. Phys. Solid State **36**, 991 (1994).

⁶ David G. Cahill and R. O. Pohl, Phys. Rev. B **35**, 4067 (1987).

⁷ F. Birch and H. Clark, *Am. J. Science* **238**, 529 (1940).

⁸ C. Kittel, Phys. Rev. **75**, 972 (1949).

⁹ J. E. Graebner, B. Golding, and L. C. Allen, Phys. Rev. B **34**, 5696 (1986).

¹⁰ A. F. Ioffe, A. R. Regel, Prog. Semicond. **4**, 237 (1960).

¹¹ S. N. Taraskin and S. R. Elliott, Phys. Rev. B **61**, 12031 (2000).

¹² H R Schober, J. Phys.: Condens. Matter, **16**, S2659 (2004).

¹³ W. Schirmacher, G. Diezemann, C. Ganter, Phys. Rev. Lett. **81**, 136 (1998).

¹⁴ S. N. Taraskin, S. R. Elliott, J. Phys.: Condens. Matter **14**, 3143 (2002).

¹⁵ W. Jin, P. Vashishta, R.K. Kalia, J.P. Rino. Phys. Rev. B **48**, 9359 (1993).

¹⁶ C. Oligschleger Phys. Rev. B **60**, 3182 (1999).

¹⁷ S. N. Taraskin, S. R. Elliott, Phys. Rev. B **56**, 8605 (1997).

¹⁸ D. G. Cahill and R. O. Pohl, Annu. Rev. Phys. Chem. **39**, 93 (1988).

¹⁹ D. G. Cahill and R. O. Pohl, Solid State Commun. **70**, 927 (1989).

²⁰ D. G. Cahill, S. K. Watson and R. O. Pohl, Phys. Rev. B **46**, 6131 (1992).

²¹ A. Einstein, Ann. Phys. **35**, 679 (1911).

²² P. B. Allen and J. L. Feldman, Phys. Rev. Lett. **62**, 645 (1989).

²³ P. B. Allen, J. L. Feldman, Phys. Rev. B **48**, 12581 (1993).

²⁴ J. L. Feldman, M. D. Kluge, P. B. Allen, F. Wooten, Phys. Rev. B **48**, 12589 (1993).

²⁵ J. L. Feldman, P. B. Allen, S. R. Bickham, Phys. Rev. B **59**, 3551 1999.

²⁶ P. B. Allen, J. L. Feldman, J. Fabian, F. Wooten, Phil. Mag. B **79**, 1715 (1999).

²⁷ P. Sheng and M. Y. Zhou, Science **253**, 539 (1991).

²⁸ P. Sheng, M. Zhou, and Zhao-Qing Zhang, Phys. Rev. Lett. **72**, 234 (1994).

²⁹ J. L. Feldman, M. D. Kluge, Phil. Mag. **71**, 641 (1995).

³⁰ Xin Yu and D. M. Leitner, Phys. Rev. B **74**, 184305 (2006).

³¹ N. Xu, V. Vitelli, M. Wyart, A. J. Liu, and S. R. Nagel, Phys. Rev. Lett. **102**, 038001 (2009).

³² N. Xu, V. Vitelli, M. Wyart, A. J. Liu, and S. R. Nagel, Phys. Rev. E **81**, 021301 (2010).

³³ Y.M. Beltukov and D.A. Parshin, Physics of the Solid State **53**, 151 (2011) (Fizika Tverdogo Tela, **53**, 142 (2011)).

³⁴ Y.M. Beltukov and D.A. Parshin, JETP Letters **93**, 598 (2011) (Pis'ma v ZhETF **93**, 660 (2011)).

³⁵ R. Bhatia. Positive Definite Matrices. Princeton University Press, Princeton (2007). 264 .

³⁶ V. Gurarie, and J.T. Chalker, Phys. Rev. B **68**, 134207 (2003).

³⁷ F. Haake, Quantum Signatures of Chaos, 2nd ed. (Springer, Berlin, 2001).

³⁸ R. N. Silver and H. Röder, Phys. Rev. E **56**, 4822 (1997).

³⁹ A. Weiße, G. Wellein, A. Alvermann, H. Fehske Rev. Mod. Phys. **78**, 275 (2006).

⁴⁰ S. N. Taraskin, Y. L. Loh, G. Natarajan, S. R. Elliott, Phys. Rev. Lett. **86**, 1255 (2001).

⁴¹ A. I. Chumakov, G. Monaco, et al. Phys. Rev. Lett. **106**, 225501 (2011).

⁴² A. Tanguy, B. Mantisi and M. Tsamados, Europhys. Lett. **90**, 16004 (2010).

⁴³ V. L. Gurevich, D. A. Parshin, J. Pelous, H. R. Schober, Phys. Rev. B **48**, 16318 (1993).

⁴⁴ D. A. Parshin and C. Laermans, Phys. Rev. B **63**, 132203 (2001).

⁴⁵ B. Rufflé, G. Guimbretière, E. Courtens, R. Vacher, and G. Monaco, Phys. Rev. Lett. **96**, 045502 (2006).

⁴⁶ B. Rufflé, D. A. Parshin, E. Courtens, and R. Vacher, Phys. Rev. Lett. **100**, 015501 (2008).

⁴⁷ F. Leonforte, R. Boissière, A. Tanguy, J. P. Wittmer, and J.-L. Barrat, Phys. Rev. B **72**, 224206 (2005).

⁴⁸ G. Monaco, S. Mossa, Proc. Natl. Acad. Sci. USA **106**, 16907 (2009);

⁴⁹ Diffusion in Condensed Matter. Methods, Materials, Models, ed. Paul Heitjans, Jörg Kärger, Springer Berlin Heidelberg New York, 2005, p.745.

⁵⁰ J. T. Edwards, D. J. Thouless, J. Phys. C. **5**, 807 (1972).

⁵¹ T. S. Grigera, V. Martin-Mayor, G. Parisi, and P. Verrocchio, J. Phys.: Condens. Matter **14**, 2167 (2002).

⁵² F. Sette, M. H. Krisch, C. Masciovecchio, G. Ruocco, G. Monaco, Science **280**, 1550 (1998).

⁵³ G. Ruocco and F. Sette, J. Phys.: Condens. Matter **13**, 9141 (2001).

⁵⁴ J. K. Christie, S. N. Taraskin, S. R. Elliott, J. Non-Cryst.Sol. **353**, 2272 (2007).

⁵⁵ B. Rufflé, M. Foret, E. Courtens, R. Vacher, G. Monaco, Phys. Rev. Lett. **90**, 095502 (2003).

⁵⁶ G. Baldi, V. M. Giordano, G. Monaco, B. Ruta, Phys. Rev. Lett. **104**, 195501 (2010).

⁵⁷ G. Baldi, V. M. Giordano, G. Monaco, Phys. Rev. B **83**, 174203 (2011).

⁵⁸ G. Baldi, V. M. Giordano, G. Monaco, B. Ruta, J.Non-Cryst.Sol. **357**, 538 (2011).

⁵⁹ B. Ruta, G. Baldi, V. M. Giordano, L. Orsingher, S. Rols, F. Scarponi, G. Monaco, J.Chem.Phys. **133**, 041101 (2010).

⁶⁰ G. Monaco, V. M. Giordano, Proc. Natl. Acad. Sci. USA **106**, 3659 (2009).

⁶¹ G. Ruocco, F. Sette, R. Di Leonardo, D. Fioretto, M. Krisch, M. Lorenzen, C. Masciovecchio, G. Monaco, F. Pignon, T. Scopigno, Phys. Rev. Lett. **83**, 5583 (1999).